# Can flocculation reduce the dispersion of deep sea sediment Plumes?

Ali, W.; Enthoven, D.H.B.; Kirichek, Alex ; Helmons, R.L.J.; Chassagne, C.

**Publication date**
2022

**Document Version**
Final published version

**Published in**
Proceedings of the World Dredging Conference, WODCON XXIII

**Citation (APA)**
Ali, W., Enthoven, D. H. B., Kirichek, A., Helmons, R. L. J., & Chassagne, C. (2022). Can flocculation reduce the dispersion of deep sea sediment Plumes? In *Proceedings of the World Dredging Conference, WODCON XXIII: Dredging is Changing* WODA.

# CAN FLOCCULATION REDUCE THE DISPERSION OF DEEP SEA SEDIMENT PLUMES?

**W. Ali[1], D. Enthoven[2], A. Kirichek[3], R. Helmons[4,5] and C. Chassagne[6]**

For green energy transition, the industry seeks alternative resources for nickel and cobalt, the main ingredients for energy storage devices and other applications. Polymetallic nodules lying at the abyssal plain are rich in these mineral resources, which leads to an increased interest in deep-sea mining (DSM) of polymetallic nodules. During the DSM operation, the seabed will be disturbed, resulting in a suspended sediment plume. Such a plume can have a significant environmental impact. As a result, defining the main processes and quantifying sediment plume dispersion is vital for predicting the possible ecological implications.

Flocculation could play a key role in minimizing and better prediction of dispersion of turbidity flows generated by deep-sea mining equipment. In this work, we study the effect of flocculation on the propagation of deep-sea sediment plumes by means of conducting a series of lock exchange experiments using artificial deep-sea sediment. Experiments were conducted in fresh and saline water with different clay and synthetic organic matter concentrations. Experiments are conducted in freshwater for comparison with saline water. The head velocity is measured via video analysis. At the end of the lock exchange experiments, subsamples at various run-out lengths are collected for particle size and settling velocity measurements. When experiments are conducted with synthetic organic matter in saline water, the results show that the head velocity reduces significantly compared to freshwater conditions due to the formation of dense flocs.

**Keywords:** Deep-sea mining, flocculation, particle size, settling velocity, plume dispersion

---

[1] Delft University of Technology,the Netherlands, w.ali@tudelft.nl.
[2] Delft University of Technology, the Netherlands, dolfenthoven@gmail.com.
[3] Delft University of Technology, the Netherlands, O.Kirichek@tudelft.nl.
[4] Delft University of Technology, the Netherlands, R.L.J.Helmons@tudelft.nl.
[5] Norwegian University of Science and Technology (NTNU), rudolfus.l.j.helmons@ntnu.no.
[6] Delft University of Technology, the Netherlands, C.Chassagne@tudelft.nl.

# 1 INTRODUCTION

Mineral and metal demand is rising as the world's population and economic activity expand. Metals and minerals, in particular, are in high need for a successful transition to green energy (e.g. wind turbines, solar panels and electric storage batteries). The most important metals are aluminium, cobalt, copper, iron, lead, lithium, nickel, and manganese (The World Bank 2017). The abyssal ocean floor is covered in polymetallic nodules, which contain significant amounts of these precious metals. The inclusion of numerous commodities in one deposit distinguishes deep-ocean nodules from terrestrial deposits; for example, nodules from the Clarion–Clipperton Zone (CCZ) largest area with polymetallic nodules (ISA, 2019; Harbour et al., 2020), contain Mn, Ni, Cu, and Co (Hein et al., 2020; Gillard, 2019). Compared to land-based deposits, deep-sea nickel, cobalt, copper, and manganese resources are substantial (Deep Green, 2018). In addition, some of the environmental issues (high CO2 emission, deforestation, toxic waste release) associated with terrestrial mining may be avoided by deep-sea mining. As a result, there is a growing interest in the polymetallic nodule's deep-sea mining (DSM).

One of the most significant environmental effects of DSM is seafloor disturbance. Seafloor sediments will be eroded during mining, resulting in a plume of suspended particles (MIDAS, 2016). Two types of plumes could be linked to DSM, the collector plume (Figure 1), generated by the mining vehicle on the seafloor (Decrop and Wachter 2019; Elerian et al., 2021) and the discharge plume after the dewatering operation of nodules on the surface vessel, consisting of water, sediment and nodule fines (Grunsven et al. 2018; Rzeznik et al. 2019; Munoz-Royo et al., 2021). The turbidity level of deep-sea water is increased by the released suspended sediment, whether it comes from the collector plume or the discharged plume, which negatively influences the marine ecosystem (Corliss, 1985; Thiel, 2003; Sharma, 2015).

The plume created by the mining vehicle (Figure 1) has the potential to have a significant environmental impact because it can spread widely (9-13 km Gillard, 2019) and stay suspended for a long time (Blue Nodules D1.7 2020; Hein et al., 2020; Roels, 1974; Oebius et al., 2001). In addition, the settling of the sediment plume and subsequent blanketing is expected to release toxic metals from the pore water, bury benthic animals, block the respiratory surfaces of filter feeders, and poison the food supply for most benthic organisms (Gollner, 2017; Jones et al., 2017; Ramirez-llodra et al., 2011; Vanreusel et al., 2016). Therefore, characterizing the primary mechanisms and quantifying sediment plume dispersion is critical for assessing the potential ecological consequences.

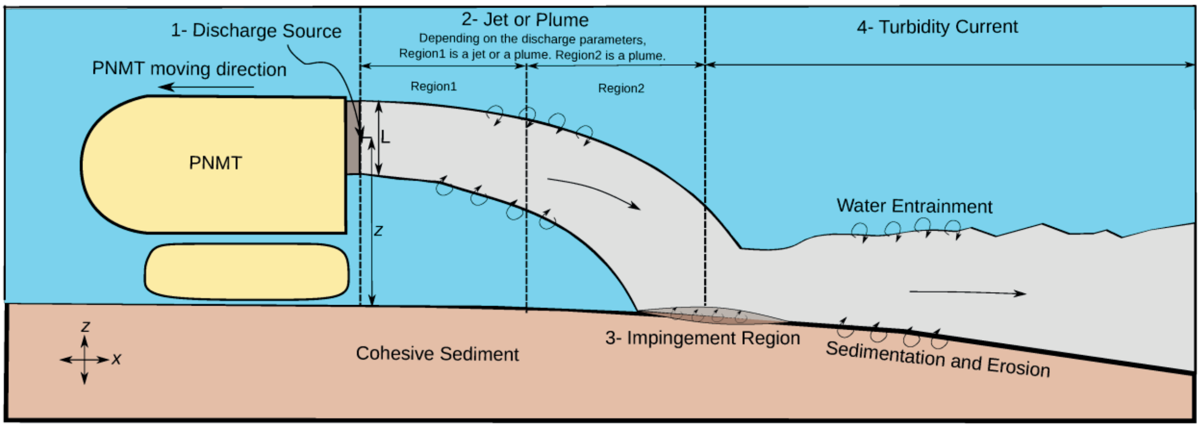

Figure 1. A schematic of how the sediment-water mixture discharged from a Polymetallic Nodule Mining Tool (PNMT) evolves (nearfield area) (Elerian et al., 2021)

Particle Size Distribution (PSD) regulates the travelling distance of deep-sea sediment plumes (Gillard et al., 2019; Spearman et al., 2020). It has been demonstrated that flocculation can potentially reduce plume dispersion since agglomerated particles can settle faster (Manning and Dyer 2002; Spearman et al., 2019; Spearman et al., 2020; Smith and Friedrichs, 2011; Gillard, 2019). Flocculation is a generic term that refers to the aggregation, break-up, and re-conformation of aggregates known as 'flocs' in various environmental conditions (Chassagne, 2020). The composition of the water in which the particles are suspended (salinity, organic matter content, sediment concentration) and the hydrodynamic conditions have a significant impact on the size, density, settling velocities and strength of flocs over time ( Manning and Dyer, 2002; Mietta, 2009; Smith and Friedrichs, 2011). Because of its high salinity and organic matter content, the deep-sea environment is ideal for flocculation. Given the environmental constraints (sediment characteristics) and tunable parameters, flocculation can help reduce plume spread. Still, optimal conditions for minimizing dispersion should be found (sediment release conditions, concentration, organic matter type and concentration).

This study aims to see how flocculation affects turbidity current propagation in the collector plume. Experiments are used to investigate how to improve flocculation and the time scales related to it.

## 2 MATERIAL AND METHODS

The clay utilized in the experiment will be called ACCZ, a lab-made artificial clay composition similar to CCZ clay. We use this material as a substitute for deep-sea sediment. The ACCZ mixture consists of two materials: i) Sibelco FT-S1 (Abidichte Ton) consisting of 64 % kaolinite, 10 % illite, 19 % quartz, and 7 % other minerals ii) Cebo OMCA Betonite consisting of 17% kaolinite, 17% illite and 66% montmorillonite. The exact percentage of these two materials is not known. The clay was made to mimic the mechanical strength of the CCZ clay. The wet ACCZ clay was placed in the oven at 105 °C for 24 hours to estimate its dry density, which was found to be 2600 kg/m$^3$. The average particle size of this clay is between 10-20 microns.

Anionic Zetag 4120 (BASF) polyelectrolyte is used in the experiments as a proxy for organic matter content. It was verified that the flocculation behavior of actual CCZ sediment is very similar to the flocculation behavior to the ACCZ. A concentration of 10mM of $CaCl_2$ is used in freshwater to create saltwater for experiments.

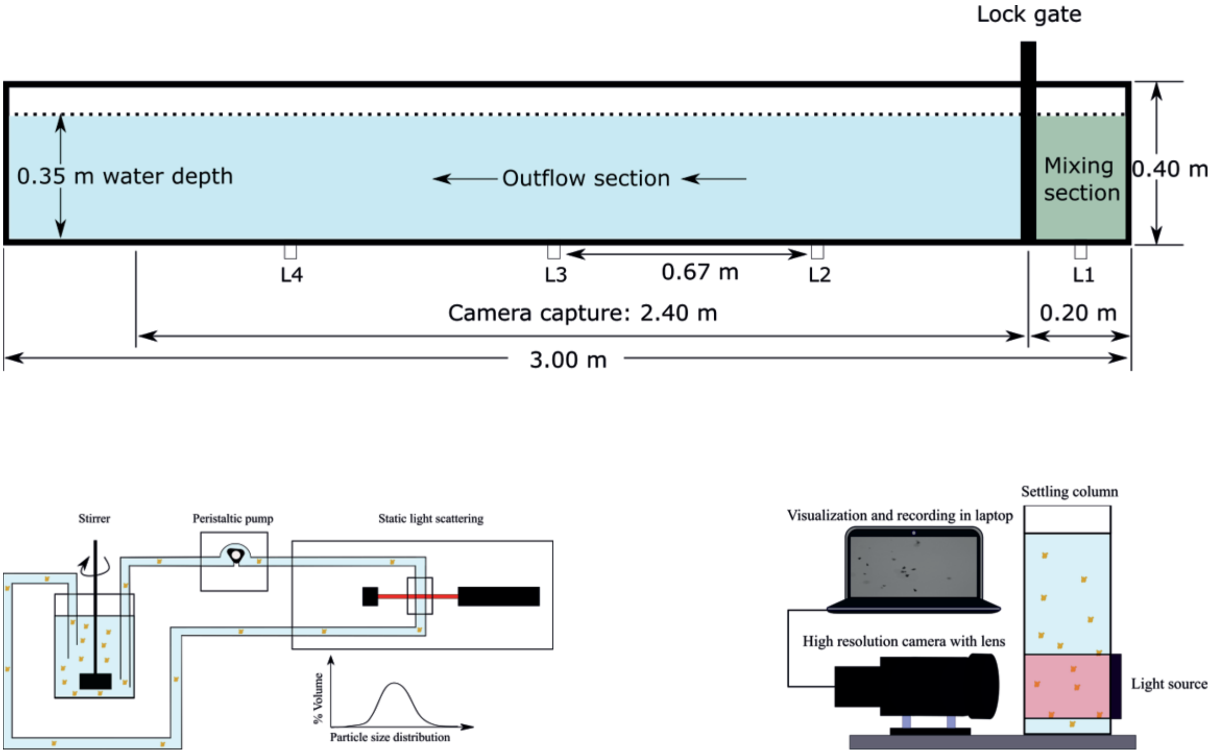

Figure 2. Schematic of experimental setups: (Top) Lock exchange. The samples are taken at L1, L2, L3 and L4 locations. (Bottom left) Particle sizer. (Bottom right) FLOCCAM

A turbidity current is generated using an experimental setup known as lock exchange (see Figure 2 top), the well-known setup used to study sediment gravity flows (Baker et al., 2017; Craig et al., 2020).

Turbidity current experiments are done both in fresh and saltwater. Two different clay concentrations (10 g/l & 30 g/l) with two flocculant dosages (0.25 mg/g & 0.75 mg/g) are used in the experiments. To generate turbidity current, ACCZ clay in dry form is mixed in water in the mixing section of the lock exchange for an hour before the lock gate is opened. One hour of mixing is enough to get a homogenous suspension with a well-defined mean particle size of 16 microns. The anionic polyelectrolyte is subsequently added and mixed for 30 seconds. Immediately after that, the lock gate is opened, the flow process is captured with the help of a high-resolution camera. The videos were shot on an IL5HM8512D: Fastec high-speed camera equipped with a Navitar 17mm lens. The camera and tank were placed beneath a dark cloth to block the outside light. The camera was placed 4.75 meters from the camera lens to the tank's front wall and films at a rate of 130 frames per second. The camera only captured the 2.40 meters left from the lock. At the end of the experiments, subsamples are collected from four locations (L1, L2, L3, L4 in figure 2 top).

The collected sub-samples are used for particle size distribution analysis with a Malvern master sizer 2000 (Figure 2 bottom left), a technique based on static light scattering (SLS). A different batch of collected sub-samples is analyzed by video microscopy using the FLOCCAM device (Shakeel et al., 2021; Ye et al., 2020; Manning et al., 2007; Mietta et al., 2009) (Figure 2 bottom right). From the videos, the flocs' size, shape, and settling velocity are determined using a custom package called Safas (MacIver 2019). The FLOCCAM can only be used for particle sizes > 20 micron.

## 3 RESULTS AND DISCUSSION

Turbidity current behaviour was significantly different in fresh and saltwater. Figure 3 shows the distance travelled by the current within the video capture range for both 10 and 30 g/l experiments. There is no noticeable difference between the experiments performed in fresh and saltwater conditions when no flocculant is added. In the absence of flocculant, turbidity currents reached the lock exchange's end irrespective of the clay concentration both in fresh and saltwater. It is known that salt-induced flocculation is slow, as flocculation, even under optimal conditions of shear, is of the order of 15-30 min (Mietta 2010). Therefore, it is not surprising that no significant effect is observed during the experimental time of the present study (less than 1 min).

Turbidity currents travelled much faster for experiments with 30 g/l as compared to 10 g/l. The results are in the same range as those obtained by Baker et al., 2017 for silica flour, kaolinite and bentonite suspensions in seawater.

The distance travelled for the experiments done in saltwater with flocculant for both clay concentrations rapidly decreased due to the effect of flocculation. As a result, the current did not reach the end of the lock exchange. In the experiments with freshwater, the current reached the end of the lock exchange (30 g/l) or nearly half the distance (10 g/l). The slight difference with the experiments performed with no flocculant can be attributed to the weak flocculation occurring in freshwater. Even though both clay and flocculant have a negative charge and are therefore expected not to flocculate, there are still enough cations in freshwater to stimulate bridging flocculation (Ibanez Sanz, 2018). In saltwater, the amount of cations is such that flocculation is promoted (Shakeel et al., 2020).

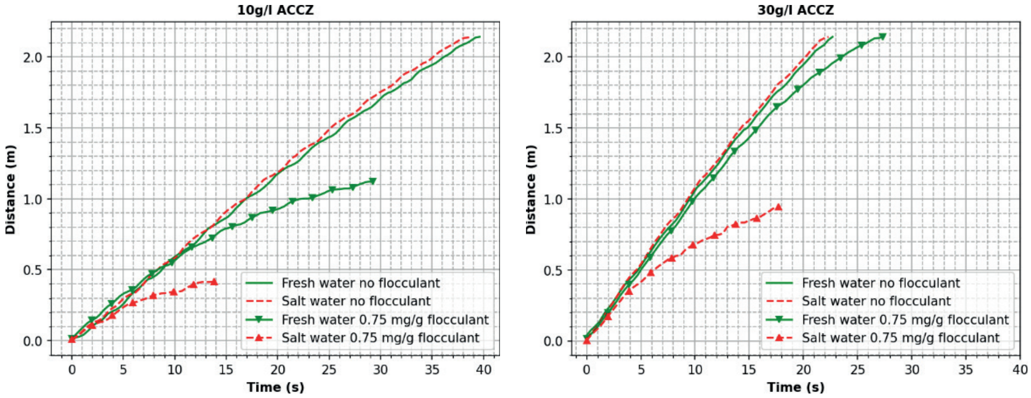

Figure 3. Change in distance as a function of time for both 10 g/l(left) and 30 g/l(right). Solid green lines represent experiments done in freshwater and dashed red lines show experiments done in saltwater. Only results with 0.75 mg/g of flocculant are shown in these figures

The floc size of the suspensions sampled at the different locations L1 – L4 are presented in Figure 4. The floc (particle) size for the experiments performed in fresh and saltwater with no added flocculant confirmed that no flocculation occurred. A mean particle size ($d_{50}$) of 22 microns was found for all locations for both experiments.

The differences between the sizes obtained from SLS and video microscopy comes from the different physics behind measuring techniques. SLS is known to "shadow" some particle sizes when a suspension is polydisperse (Ibanez Sanz, 2018), resulting in the fact that the number of large particles can be artificially higher than in reality. Therefore, it is expected that the results obtained from the FLOCCAM, which is based on a statistical analysis of particle size, are more accurate in the range (20-1000) microns. The bars given in Figure 4 represent the standard deviation around the mean floc size. It is clear, seen in the large bars, that the samples are polydisperse.

It is found that flocs in freshwater are larger than flocs created in saltwater for 30 g/l with 0.75mg/g of flocculant (see Figure 4). The reason is that in freshwater, the polyelectrolyte is less coiled than in saltwater due to the electrostatic repulsion between the charged groups on the polymer backbone. Therefore, denser flocs are created with anionic flocculant in saltwater.

The floc size for the experiment with flocculant in saltwater is shown at only two locations because the turbidity current settles after L2 (as is also apparent in Figure 3).

The settling velocities and particle size range for 30 g/l ACCZ with 0.75 mg/g of flocculant at the locations L1 and L4 (for freshwater) and L1 and L2 (for saltwater) are shown in Figures 5 and 6. The settling velocities are smaller in the freshwater case compared to the saltwater case, at the position where the turbidity current settles down. This behaviour is correlated with the fact that the flocculant is more uncoiled in freshwater than in saltwater: in saltwater, flocs are denser and have a higher settling velocity. The settling behaviour and floc size are not changing between L1 and L2 for the saltwater sample, implying that, as expected, optimal flocculation has occurred in the mixing tank. Thanks to the cations present in saltwater, the bridging between anionic polyelectrolyte and clay is complete.

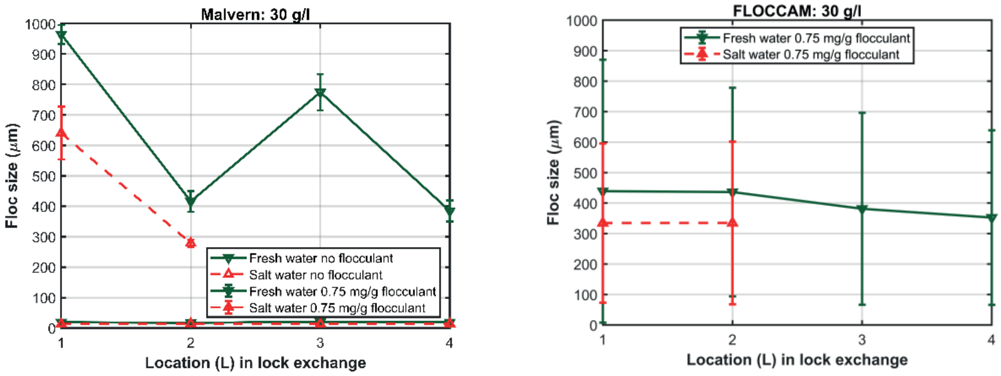

Figure 4. Hydrodynamic diameter for 30 g/l experiments at different locations (L1-L4) in the lock exchange. Solid green lines represent experiments done in freshwater and dashed red lines show experiments done in saltwater. Only results with 0.75 mg/g of flocculant are shown in these figures

For the freshwater sample, it is most probable that the flocculation in the mixing tank is incomplete due to a lack of cations. However, the formed flocs have the same properties (same size, same settling velocity) as flocs formed in saltwater conditions, as proven by the similarity between the distributions in L1 (Figures 5 and 6). When the lock is opened, flocs, clay particles and unbounded flocculant are released. The clay particles and unbounded flocculant come into contact with freshwater that contains cations. These cations can act as a binding agent, and therefore flocculation can occur. Flocculation by polyelectrolyte is very fast and of the order to seconds (Shakeel et al., 2020; Ibanez Sanz, 2018).

Consequently, flocs are formed, leading to a shift in particle size as observed between L1 and L4. In particular, it is found that quite some flocs formed during the propagation of the turbidity current are elongated, resulting in flocs of large equivalent diameter (shown by the red circle in the bottom panels of Figure 5). These large flocs have a very low settling velocity as they are made of low density uncoiled flocculant to which some clay is bound. These flocs can be seen in the snapshot in Figure 5. Due to their short residence time in the water column, these flocs could not capture more clay particles and did not have time to coil. Coiling of flocs occurs over more extended periods of time when turbulent shear make the dangling ends of the polyelectrolyte collapse onto the floc. The flocs then become rounder and denser (Shakeel et al., 2020). Similar results were obtained for the 10 g/l experiments with 0.75 mg/g flocculant.

## 4 CONCLUSION

In this work, we investigated the effect of flocculation on the turbidity current inside a lock exchange and the time scale associated with flocculation. We showed that it is necessary to have a flocculating agent to induce flocculation. In nature, this flocculating agent would be organic matter. We used an anionic polyelectrolyte as a proxy for organic matter in the laboratory. It was shown that flocs are created a few seconds after adding synthetic organic matter in fresh and saltwater conditions. As a result, the turbidity current settled faster. This also shows that flocculation can be expected when organic matter is present in a saline deep-sea environment. This organic matter is usually composed of organic debris and exopolymers excreted by microorganisms.

Further research will indicate which specific type and concentration of organic matter are required to significantly reduce plume dispersion. Even though this research is performed in the frame of deep-sea mining, the results presented here are very general and could be applied to a large variety of dredging plumes. In particular, we showed that even in freshwater conditions, where flocculation is expected to be difficult owing to the electrostatic repulsion between organic matter and clay, flocculation can be observed. This implies that models for dredging plumes dispersions should be revised to account for flocculation.

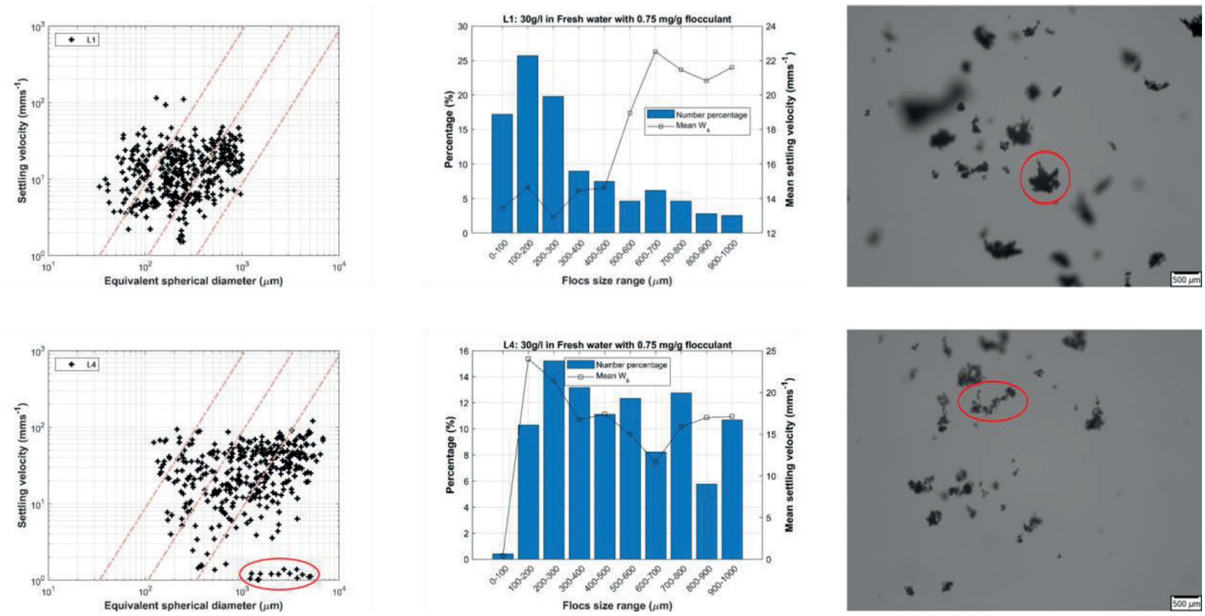

Figure 5. Settling velocity and particle size analysis of the subsamples collected at location L1 (top panels) and L4 (bottom panels) during lock exchange experiments with 30 g/l ACCZ and 0.75 mg/g of flocculant in freshwater. Settling velocity is derived as a function of equivalent spherical diameter, with diagonal dashed lines representing the contours of effective density (kg m$^{-3}$). Middle panels show floc size range and mean settling velocity. The images of the flocs are given in the right panels

## ACKNOWLEDGEMENTS

This work is performed in the framework of PlumeFloc (TMW.BL.019.004, Topsector Water&Maritiem: Blauwe route) within the MUDNET consortium. The authors would like to thank Deltares for using their experimental facilities in the framework of the MoU between MUDNET / Deltares. In addition, we thank Ahmad Shakeel (Delft University of Technology), Michael R. MacIver (The University of British Columbia) and Paul J.M. van Kan (Van Kan Scientific) for their useful insight regarding the use of FLOCCAM and Safas.

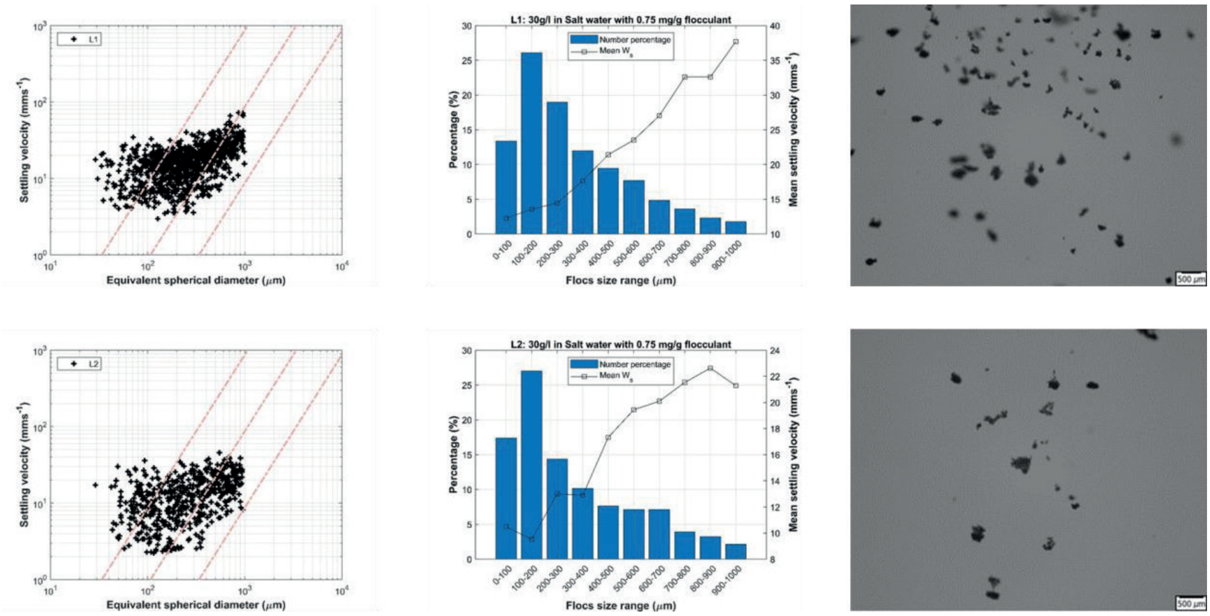

Figure 6. Settling velocity and particle size analysis of the subsamples collected at location L1 (top panels) and L2 (bottom panels) during lock exchange experiments with 30 g/l ACCZ and 0.75 mg/g of flocculant in saltwater. Settling velocity is derived as a function of equivalent spherical diameter, with diagonal dashed lines representing the contours of effective density (kg m$^{-3}$). Middle panels show floc size range and mean settling velocity. The images of the flocs are given in the right panels

## REFERENCES

**Baker M.L., Baas J.H., Malarkey J., Jacinto R.S., Craig M.J., Kane I.A. & Barker S.** (2017). The Effect of Clay Type On the Properties of Cohesive Sediment Gravity Flows and Their Deposits, *Journal of Sedimentary Research,* 87, 11, 1176–1195.

**Blue Nodules D1.7** (2020). Environmental Impact Assessment (EIA) components for test mining up to prototype level (TRL 6), *Technical report*.

**Chassagne C.** (2020). Introduction to Colloid Science, *Delft Academic Press*, ISBN 9789065624376. https://books.open.tudelft.nl/home/catalog/book/16.

**Corliss B.H.** (1985). Microhabitats of benthic foraminifera within deep-sea sediments. *Nature*, 314, 4–7.

**Craig M.J., Baas J.H., Amos K.J., Strachan L.J., Manning A.J., Paterson D.M., Hope J. A., Nodder S.D. & Baker M. L.** (2020). Biomediation of submarine sediment gravity flow dynamics, *Geology*, 48, 1, pp. 72-76, https://doi.org/10.1130/G46837.1.

**Cuyvers L., Berry W., Gjerde, K., Thiele, T. & Wilhem C.** (2018). Deep Seabed Mining: A Rising Environmental Challenge, *IUCN and Gallifrey Foundation*: Gland, Switzerland.

**Decrop B. & Wachter T.D.** (2019). Detailed CFD Simulations For near Field Dispersion of Deep Sea Mining Plumes, *In Proceedings of the World dredging conference (WODCON XXII)*, Shanghai, China, 22–26, 116–127.

**Deep Green**. (2018). 43-101 Technical Report for the NORI Clarion – Clipperton Zone Project, Pacific Ocean, *Technical report*.

**Elerian M., Alhaddad S., Helmons R. & Van Rhee C.** (2021). Near-Field Analysis of Turbidity Flows Generated by Polymetallic Nodule Mining Tools. *Mining* 2021, 1, 251-278. https://doi.org/10.3390/mining1030017.

**Gillard B.** (2019). Towards Deep Sea Mining-Impact of mining activities on benthic pelagic coupling in the Clarion Clipperton Fracture Zone. *PhD Thesis*, Universität Bremen.

**Gillard B., Purkiani, K., Chatzievangelou, D., Vink A., Iversen M.H. & Thomsen L.** (2019). Physical and hydrodynamic properties of deep sea mining-generated, abyssal sediment plumes in the Clarion Clipperton Fracture Zone (eastern-central Pacific). *Elementa*, 7, 5.

**Gollner S., Kaiser S., Menzel L., Jones D.O.B., Brown A., Mestre N.C., Oevelen D.V., Menot L., Cola A., Canals M., Cuvelier D., Durden J.M., Gebruk A., Egho G.A., Haeckel M., Marcon Y., Mevenkamp L., Morato T., Pham C.K., Purser A., Sanchez-vidal A., Vanreusel A., Vink A. & Martinez P.** (2017). Resilience of benthic deep-sea fauna tomining activities, *Marine Environmental Research*, 129:76–101.

**Grunsven F., Keetels G. & Van Rhee C., (2018).** The Initial Spreading of Turbidity Plumes—Dedicated Laboratory Experiments for Model Validation. In Proceedings of the *47th Underwater Minerals Conference*, Bergen, Norway.

**Harbour P.R., Leitner A.B., Ruehlemann C., Annemiek V. & Sweetman A.K.** (2020). Benthic and Demersal Scavenger Biodiversity in the Eastern End of the Clarion-Clipperton Zone – An Area Marked for Polymetallic Nodule Mining, *Frontiers in Marine Science*, 1–14.

**Hein J.R., Koschinsky A. & Kuhn. T.** (2020). Deep-ocean polymetallic nodules as a resource for critical materials. *Nature Reviews Earth and Environment*, 1, 3, 158–169.

**Ibanez Sanz M.** (2018). Flocculation and consolidation of cohesive sediments under the influence of coagulant and flocculant. *PhD Thesis,* Delft University of Technology.

**ISA** (2019). Current Status of the Reserved Areas With the International Seabed Authority [WWW Document], *Technical report*.

**Jones D.O.B., Kaiser S., Sweetman A.K., Smith C.R., Menot L., Vink A., Trueblood D., Greinert J., Billett D.S.M., Arbizu P.M., Radziejewska T., Singh R., Ingole B., Durden J.M., Clark M.R., Stratmann T. & Simon-lledo E.** (2017). Biological responses to disturbance from simulated deep-sea polymetallic nodule mining, *PLOS ONE,* 12, 2, e0171750.

**MacIver M.R.** (2019). Development and usability assessment of a connected resistance exercise band application for strength-monitoring, *World Acad. Sci. Eng. Technol,* 13, 340–348, https://doi.org/10.5281/zenodo.

**Manning A.J. & Dyer K.R.** (2002) A Comparison Of Floc Properties Observed During Neapand Spring Tidal, *Proceedings in Marine Science*, 233–250.

**Manning A., Friend P., Prowse N. & Amos C.** (2007). Estuarine mud flocculation properties determined using an annular mini-flume and the LabSFLOC system, *Continental Shelf Research*, 27, 8, 1080-1095.

**MIDAS** (2016). Implications of MIDAS results for policy makers: recommendations for future Regulations.

**Mietta F., Chassagne C., Manning A.J. & Winterwerp J.C.** (2009). In-fluence of shear rate, organic matter content, pH and salinity on mud flocculation, *Ocean Dynamics*, 59, 5, 751–763.

**Mietta F.** (2010). Evolution of the floc size distribution of cohesive sediments, *PhD Thesis,* Delft University of Technology.

**Munoz-Royo C., Peacock T., Alford M.H., Smith J.A., LeBoyer A., Kulkarni C.S., Lermusiaux P.F.J., Haley P.J., Mirabito C., Wang D., Adams E.E., Ouillon R., Breugem A., Decrop B., Lanckriet T., Supekar R.B., Rzeznik A.J., Gartman A. & Ju S.J.** (2021). Extent of impact of deep-sea nodule mining midwater plumes is influenced by sedimentloading, turbulence and thres holds, *Communications Earth Environment*, 2, 1.

**Oebius H. U., Becker H.J., Rolinski S. & Jankowski J.A.** (2001). Parametrization and evaluation of marine environmental impacts produced by deep-sea manganese nodule mining, *Deep-Sea Research Part II*, 48, 3453–3467.

**Ramirez-llodra E., Tyler P.A., Baker M.C., Bergstad O.A., Clark M.R., Levin L.A., Menot L., Rowden A.A., Smith C.R. & Dover C.L.V.** (2011). Man and the Last Great Wilderness: Human Impact on the Deep Sea, *PLOS ONE,* 6, 8, e22588.

**Roels O.,** (1974). Environmental Impact of Manganese Nodule Mining, *Technical report*.

**Rzeznik A.J., Flierl G.R. & Peacock T.** (2019). Model investigations of discharge plumes generated by deep-sea nodule mining operations. *Ocean Engineering*, 172, 684–696.

**Shakeel A., MacIver M.R., van Kan P.J.M., Kirichek A. & Chassagne C.** (2021). A rheological and microstructural study of two-step yielding in mud samples from a port area. *Colloids and Surfaces A: Physicochemical and Engineering Aspects,* 624, 126827.

**Shakeel A., Safar Z., Ibanez Sanz M., Van Paassen L. & Chassagne C.** (2020). Flocculation of clay suspensions by anionic and cationic polyelectrolytes: A systematic analysis. *Minerals*, 10, 999, https://doi.org/10.3390/min10110999.

**Sharma R.** (2015). Environmental issues of deep-sea mining. *Procedia Earth Planetary Science*, 11, 204–211.

**Smith S.J. & Friedrichs C.T.** (2011). Size and settling velocities of cohesive flocs andsuspended sediment aggregates in a trailing suction hopper dredge plume, *Continental Shelf Research*, 31(10 SUPPL.), S50–S63.

**Spearman J., Taylor J., Crossouard N., Cooper A., Turnbull M., Manning A., Lee M. & Murton B.** (2020) Measurement and modelling of deep sea sediment plumes and implications for deep sea mining. *Scientific Reports*, 10, 1, 1–14.

**Spearman J., Taylor J., Crossouard N., Cooper A., Turnbull M., Manning A. & Lee M.** (2019). The measurement and modelling of plumes resulting from deep sea mining of Fe-Mn Crusts, *In Proceedings of the World dredging conference (WODCONXXII)*, Shanghai, China.

**The World Bank** (2017). The Growing Role of Minerals and Metals for a Low Carbon Future. *Tech. rep.* June. DOI: 10.1596/28312.

**Thiel H.** (2003). Anthropogenic impacts on the deep sea, in: Tyler, P.A. (Ed.) Ecosystems of the deep oceans, *Ecosystems of the World*, 28, 427-471.

**Vanreusel A., Hilario A., Ribeiro P.A. & Menot L.** (2016). Threatened by mining, polymetallic nodules are required to preserve abyssal epifauna, *Nature Publishing Group*, 1–6.

**Ye L., Manning A.J. & Hsu T.J.** (2020). Corrigendum to ”Oil-mineral flocculation and settling velocity in saline water”, *Water Research*, 173, 115569.